The most stable crystal structure and the formation processes of an order-disorder (OD) intermetallic phase in the Mg-Al-Gd ternary system

K. Kishida[a,b,*], H. Yokobayashi[a], and H. Inui[a,b]

[a] *Department of Materials Science and Engineering, Kyoto University, Sakyo-ku, Kyoto, 606-8501 JAPAN*
[b] *Center for Elements Strategy Initiative for Structure Materials (ESISM), Kyoto University, Sakyo-ku, Kyoto, 606-8501 JAPAN*

The most stable crystal structure for an 18R-type order-disorder (OD) intermetallic phase in the Mg-Al-Gd ternary system and its formation processes by annealing at 525 °C have been investigated by means of transmission electron microscopy (TEM) and scanning transmission electron microscopy (STEM). The most energetically favourable polytype at 525 °C is found to be the structurally simplest one, a maximum degree of order (MDO) polytype (monoclinic, 1M, space group: $C2/m$) that is described with a single stacking vector in stacking six-layer structural blocks. The formation of this simplest polytype occurs in the sequence of (i) enrichment of Gd and Al in four consecutive close-packed planes while keeping the hcp stacking of the AB-type, (ii) formation of Al_6Gd_8 clusters in the four consecutive atomic planes, introducing a stacking fault in the middle of the four consecutive atomic planes, (iii) thickening by the formation of Gd and Al-enriched four consecutive planes at a distance of two or three close-packed Mg atomic planes from the pre-existing Gd and Al-enriched four consecutive atomic planes so as to form 6-layer and sometimes 7-layer structural blocks, (iv) in-plane ordering of Al_6Gd_8 clusters in the four consecutive atomic planes and the stacking of structural blocks in the preferential stacking positions to form the OD structure, and (v) elimination of different structural blocks (other than 6-layer ones) and the long-range ordering in the stacking of structural blocks.

Keywords; magnesium alloys; scanning transmission electron microscopy (STEM); crystal structure; long period stacking ordered structure; order-disorder (OD) theory

1. Introduction

Mg alloys containing TM (Transition-metal) and RE (Rare-earth) elements have received a considerable amount of attention in recent years as a new-class of light-weight structural material that exhibits high strength and high ductility simultaneously [1-6]. Although detailed mechanisms for endowing such attractive mechanical properties and high ductility with these Mg alloys have largely been remained unsolved, ternary Mg-TM-RE precipitate phases with a long-period stacking- ordered (LPSO) structure have been believed to play a role [1-6]. Crystal structure refinement for these ternary LPSO phases is indispensable for deducing the mechanism behind the simultaneous achievement of the attractive mechanical properties and there have indeed been many studies on the subject by phase-contrast high-resolution (HR) transmission electron microscopy (TEM) [7-10] and scanning transmission electron microscopy (STEM) [11-17]. We have very recently investigated the crystal structures of the LPSO phase corresponding to the 18R polytype newly found in the Mg-Al-Gd system by means of STEM [13,14] and found the following facts: first, the enrichment of RE and

TM atoms occurs in four consecutive close-packed atomic planes in each structural block consisting of six atomic planes, and, second, the long-range atomic ordering involving a periodic arrangement of Al_6Gd_8 clusters of the $L1_2$ type occurs in the RE and TM-enriched four consecutive atomic planes, in which a stacking fault that disturbs the hexagonal close-packed (hcp) stacking of the AB-type occurs. Because of these characteristics, the LPSO phase in the Mg-Al-Gd system cannot be described as 'LPSO' phase any longer in a strict sense and the crystal structure is described with the concept of the order-disorder (OD) structure. In the framework of the theory of the OD structure, a crystal structure is described with the symmetry of a structural block (an OD layer) and the relative relation between adjacent two OD layers [14,15,18-24], as the details are described in the next section. When two or more stacking relations between adjacent two OD layers are crystallographically equivalent with respect to the symmetry of the OD layer, many different polytypes as well as virtually one-dimensionally disordered structures along the stacking direction can be formed as frequently observed in many minerals and ceramics such as wollastonite and SiC [20,22-24]. Then, questions arise as to whether there is a particular polytype that is the most energetically favourable, how the most energetically favourable polytype correspond to the crystallographically simplest structure, and what determines the most energetically favourable polytype. Questions arise also as to in what sequence the precipitation process of the most energetically favourable polytype proceeds with some possible elementary processes such as the enrichment of RE and TM atoms in four consecutive atomic planes, the introduction of stacking faults in the RE and TM-enriched atomic layers, the formation of Al_6Gd_8 clusters and their in-plane ordering, the formation of structural blocks, the stacking of these structural blocks and so on.

In the present study, we investigate the variation of the crystal structure of the OD intermetallic phase in the Mg-Al-Gd system with annealing at a high temperature (525 °C) by means of transmission electron microscopy (TEM) and scanning transmission electron microscopy (STEM), in order to elucidate the crystal structure corresponding to the most energetically favourable polytype and the formation process of the most energetically favourable OD structure.

2.   OD structure

The theory of the OD structure (OD theory) was originally developed to describe crystal structures with one-dimensional stacking disorder observed in many minerals, such as wollastonite [18-24]. In the OD theory [18-24], a crystal structure is described with two sets of partial operations (POs) of symmetry, λ-POs and σ-POs. The λ-POs correspond to POs that transform an OD layer into itself, while σ-PO transforms an OD layer into an adjacent one above it. For a given set of λ-POs, i.e. a given layer group, a set of σ-POs can be derived based on the symmetry of the layer group. A whole family of the derivative structures described with a complete set of POs is called an OD-groupoid family. We have recently determined the OD-groupoid family for the 18R-type OD intermetallic compound in the Mg-Al-Gd system [14]. The 18R-type OD intermetallic phase is found to form by stacking structural blocks, each of which consists of six close-packed atomic planes. In each of these structural blocks, Gd- and Al-enriched four consecutive atomic planes are inserted between two pure Mg layers and a stacking fault that disturbs the hcp stacking of the AB-type is introduced in the middle of the Gd- and Al-enriched four consecutive atomic planes.

The in-plane long-range ordering in the Gd- and Al- enriched four consecutive planes in each structural block can be described as a periodic arrangement Al_6Gd_8

clusters with the L1$_2$-type atomic arrangement on lattice points of a two-dimensional $2\sqrt{3}a_{\mathrm{Mg}} \times 2\sqrt{3}a_{\mathrm{Mg}}$ primitive hexagonal lattice, where a_{Mg} is referred to the length of the unit vector along the a-axis of Mg (Fig. 1(a)). For the OD intermetallic phase, the 6-layer structural block corresponds to the OD layer with the layer group symmetry of $P(3)1m$ [14,25]. Three different OD-groupoid families can be derived for the OD intermetallic phase depending on stacking relations between neighbouring OD layers [14,15]. These three OD-groupoid families are described with three different types of stacking positions (C$_1$-C$_3$ in Fig. 1(b)) that are reduced from 12 different positions of the structural block by symmetry consideration [14]. Among three possible OD-groupoid families, the 18R-type OD intermetallic phase is revealed to form an OD-groupoid family described with the C$_1$ stacking position. There are three crystallographically equivalent positions for the C$_1$ position as described with the stacking vectors,

$$t_1 = -\frac{1}{3}a_1 + h \tag{1a}$$

$$t_2 = -\frac{1}{3}a_2 + h \tag{1b}$$

$$t_3 = \frac{1}{3}(a_1 + a_2) + h \tag{1c}$$

where a_1 and a_2 correspond to the unit vectors of the structural block in the hexagonal setting and h corresponds to the unit vector of the 6-layer structural block along the stacking direction. Many different polytypes belonging to a single OD-groupoid family can be deduced by assuming different combinations of stacking vectors described in eqs. (1a)-(1c). In any OD-groupoid family, there exist some structurally simple polytypes, designated as polytypes with the maximum degree of order (MDO polytypes) [19,20,22-24]. Three MDO polytypes, 1M (MDO1, space group: $C2/m$), 2M (MDO2, space group: $C2/c$) and 3T (MDO3 and MDO3', enantiomorphic space group pair: $P3_112$ and $P3_212$) in the Ramsdell notation, are deduced for the OD-groupoid family by considering some simple combinations of the stacking vectors (1a)-(1c) [14,15], as will be described in some more detail in the 4.1. section.

Structural characteristics of OD structures can be extracted by inspecting their electron diffraction patterns. For crystals belonging to a single OD-groupoid family, reflections are classified into two types; OD 'family' reflections that appear at identical positions to all possible polytypes belonging to the OD-groupoid family, and 'characteristic' reflections that appear at different positions depending on polytypes [14,15,23,24]. This indicates that the identification of the OD-groupoid family can be made by inspecting positions of family reflections, while that of polytype belonging to a given OD-groupoid family can be made by inspecting those of characteristic reflections. Fig. 2 shows electron diffraction patterns calculated for some simplest (MDO) polytypes (1M, 2M and 3T) of the OD-groupoid family of the 18R-type OD intermetallic compounds in the Mg-Al-Gd system with NCEMSS software [26] for the incident beam directions corresponding to [2$\bar{1}$10][†] and [1$\bar{1}$00] of Mg with the hcp

---

[†]Since the OD phase is known to form in the Mg matrix so that their close-packed directions and planes are parallel to each other, Miller indices to express directions and planes for the OD phase are referred to as those of the matrix phase of Mg with the hcp structure unless otherwise stated.

structure. Reciprocal lattice rows of family and characteristic reflections are indicated with two-headed and one-headed arrows in the figure, respectively. If the three crystallographically equivalent stacking relations (eqs. (1a)-(1c)) occur randomly in stacking 6-layer structural blocks (OD layers), the OD phase exhibits a one-dimensionally disordered nature. Then, reciprocal lattice rows of the characteristic reflections exhibit virtually sharp streaks extending along the stacking direction, while those of the family reflections appear as discrete spots. If stacking positions other than C_1 (i.e., 'non-equivalent stacking' described with positions C_2 and C_3 in Fig. 1(b)) are taken in addition to those of C_1 in their stacking, some OD structures belonging to different OD-groupoid families are incorporated. Then, streaks are expected to occur along reciprocal lattice rows of both family and characteristic reflections for the OD phase. However, in this particular case, $n[01\bar{1}l]^*$ and $n[11\bar{2}l]^*$ reciprocal lattice rows (n: integer) of the family reflections are confirmed to be common to all three OD-groupoid families described either C_1, C_2 or C_3 positions. Therefore, these rows of the family reflections keep exhibiting discrete spots, while other rows of the family reflections exhibit streaks along the stacking direction, when identical 6-layer structural blocks stack on each other taking positions more than two of C_1, C_2 and C_3 positions. If, on the other hand, structural blocks consisting of different numbers of close-packed planes are incorporated (intergrowth), streaks are expected to occur along reciprocal lattice lows of both family and characteristic reflections for the OD phase, as in the case of the incorporation of the hcp structure in the face-centered cubic (fcc) structure and vice versa.

3.   Experimental procedures

Ingots of a Mg-Al-Gd ternary alloy were produced by high-frequency induction-melting mixtures of high-purity Mg, Al and Gd amounting to a nominal composition of Mg - 3.5 at.%Al - 7.0 at.%Gd in a carbon crucible with a lid in vacuum. After melting, the ingot was quickly removed from the furnace to observe the as-solidified microstructures. Then, the ingot was annealed at 525 °C for various periods of time ranging from 4 to 64 hours followed by water-quenching. Microstructures were examined by scanning electron microscopy (SEM), TEM and STEM with JEOL JEM-2000FX and JEM-2100F electron microscopes operated at 200 kV. Chemical compositions were analyzed by energy dispersive x-ray spectroscopy (EDS) in the SEM. Specimens for SEM, TEM and STEM observations were cut from as-solidified and annealed ingots, mechanically polished and electropolished in a solution of nitric acid and methanol (9:21 by volume) under a constant voltage of 17 V at -55 °C.

4.   Results

4.1. SEM observations

The as-solidified ingot exhibits inhomogeneous microstructures depending on ingot position. The lower and upper parts of the ingot have average chemical compositions of Mg-10 at.%Al-9 at.% Gd and Mg-1 at.%Al-5 at.% Gd, respectively. The lower part (Al-rich region) is composed of three phases; Mg, $GdMg_5$ and Al_2Gd with a (Mg + $GdMg_5$) eutectic microstructure being formed from place to place. The upper part exhibiting an Al-poor composition additionally contains the Mg-Al-Gd OD intermetallic phase that appears as thin plates in the (Mg + $GdMg_5$) eutectic microstructure, as seen in a SEM backscattered electron image in Fig. 3(a). The formation process and crystal structure

evolution of the Mg-Al-Gd OD intermetallic phase was investigated by examining the microstructures in the upper part of the ingot throughout the present study.

Typical microstructures in the upper part of the ingot annealed at 525 °C for 4 and 64 hours are depicted in Figs. 3(b) and (c), respectively. As the annealing time is increased, the volume fraction for the OD intermetallic phase increases slightly while those for Al_2Gd (the brightest phase) and $GdMg_5$ (the second brightest phase) decrease significantly. As a result, the alloy is basically composed of three phases, the OD intermetallic phase, Mg and Al_2Gd after annealing at 525 °C for 64 hours. Based on the TEM/STEM analyses described below, the increase of volume fraction of the OD intermetallic phase appears to occur not only by the thickening of the pre-existing plates but also by the nucleation of new precipitates plates during annealing.

4.2. TEM and STEM observations

4.2.1. Early stage of the formation processes of the OD intermetallic phase

Figure 4(a) shows a low-magnification bright-field (BF)-TEM image taken along [$2\bar{1}\bar{1}0$] of an OD intermetallic precipitate with a thickness about 1.5 μm (when measured along the stacking direction) observed in an as-solidified specimen. Many bright lines running horizontally in the image (marked with arrows) correspond to positions where stacking irregularity occurs. The number of atomic layers in most structural blocks is six in most areas of the imaged OD intermetallic precipitate, especially in areas well within the precipitate. The stacking irregularities observed in Fig. 4(a) are confirmed to form by the introduction of structural blocks with different numbers of constituent atomic layers (i.e., intergrowth), as shown in an atomic-resolution HAADF-STEM image of Fig. 4(b). Atomic resolution HAADF-STEM images of 18R-type stacking regions based on 6 atomic-layer structural blocks (well within relatively thick (about 1.5 μm) OD intermetallic precipitates) taken along [$2\bar{1}\bar{1}0$] and [$1\bar{1}00$] are shown in Figs. 5(a) and (d), respectively. Although the arrangement of brighter spots corresponding to that of Gd-enriched atomic columns varies from place to place in the HAADF-STEM images of the [$2\bar{1}\bar{1}0$] and [$1\bar{1}00$] incidences (Fig. 5(a) and 5(d)), most regions are already composed of the 6-layer structural blocks with the ABACBC-type stacking and the Gd-enrichment evidently occurs already in the central four consecutive layers with the fcc-type stacking (Fig. 5(a-c). The ordered arrangement of brighter spots identical to that observed previously in the OD intermetallic phase in the well-annealed alloy (Fig. 3(a) and 3(b) in ref. 14) is clearly seen in some areas (Fig. 5(b) and 5(e)), while such ordering of brighter spots is less evident in other areas (Fig. 5(c) and 5(f)). In the HAADF-STEM image of the [$1\bar{1}00$] incidence (Fig. 5(d)), intensities of the Gd-enriched columns and the interval of the adjacent Gd-enriched columns in the outer Gd-enriched atomic layers vary significantly. All these observations indicate that the formation of Al_6Gd_8 clusters with the fcc-based $L1_2$-type atomic arrangement already occurs at this stage but that the long-range in-plane ordering of these Al_6Gd_8 clusters has not completed yet.

SAED patterns of the OD intermetallic precipitate of Fig. 4(a) taken along [$2\bar{1}\bar{1}0$] and [$1\bar{1}00$] directions are shown in Fig. 6(a) and (b), respectively. These SAED patterns were taken from an area well within the precipitate with a selected-area aperture of 0.13 μm in diameter. In both patterns, superlattice spots are observed in the 000l systematic row at positions dividing the distance between the transmitted beam and 0002 fundamental reflection (corresponding to the interplanar spacing of close-packed planes) by six, indicating that the number of close-packed atomic planes comprising

each of structural blocks is mostly six, as confirmed by atomic-resolution HAADF-STEM imaging (Figs. 4 and 5). The reciprocal lattice rows of $n/2[01\bar{1}l]^*$ (n: odd integer) and $n/6[11\bar{2}l]^*$ ($n \neq 6m$, m = integer) exhibit diffuse nature, which is due mainly to the fact that the in-plane ordering of Al_6Gd_8 clusters is not completed yet in the OD phase at this stage of precipitation, as observed in the atomic-resolution HAADF-STEM image (Fig. 5). In addition, weak streaks are observed in all reciprocal lattice rows of $n/2[01\bar{1}l]^*$ and $n/6[11\bar{2}l]^*$ (n = integer) regardless of whether they are the family or characteristic reflection rows. This is due to minor incorporation of structural blocks composed of different numbers of close-packed atomic planes (Fig. 4).

In as-solidified ingots, very thin precipitates of the OD phase consisting only of one structural block or two are also often observed. A typical example of low-magnification HAADF-STEM image of these thin OD precipitates taken along $[2\bar{1}\bar{1}0]$ is shown in Fig. 7(a), in which each bright line observed horizontally corresponds to one set of Gd-enriched four consecutive atomic layers in one structural block. Very thin precipitates of the OD phase consisting only of one and two structural blocks are marked with A and B in Fig. 7(a), respectively. Close examination of Fig. 7(a) indicates that faint lines with a similar thickness appears next to the bright lines at a distance corresponding to either six or seven atomic layers. This suggests that enrichment of Gd and Al atoms occurs also in the close vicinity of very thin precipitates as a thickening process along the stacking direction.

Atomic-resolution HAADF-STEM images of these very thin OD precipitates taken along $[2\bar{1}\bar{1}0]$ together with their horizontally averaged intensity profiles are depicted in Figs. 8(a)-(c). The number of structural blocks of each of thin OD precipitates is one for Fig. 8(a) and two for Figs. 8(b) and (c). In the Gd-enriched four consecutive atomic planes, an ordered arrangement of brighter spots (Gd-enriched atomic columns) characteristic to the ordered arrangement of Al_6Gd_8 clusters is observed to be developing. Since two and three Mg atomic planes exist between two sets of four-consecutive Gd-enriched atomic planes in Figs. 8(b) and (c), these two thin precipitates are regarded as nuclei for the OD phases of the 18R- and 14H-types, respectively. In the close vicinities of these nuclei, atomic planes exhibiting slightly brighter intensity appear, being separated by two or three atomic planes of nearly pure Mg. Each of these corresponds to one of the faint lines located next to the brightest lines in Fig. 7(a). As marked in Figs. 8(a)-(c), the enrichment of Gd atoms in the faint lines occurs roughly in four consecutive atomic planes. Of importance to notice in Figs. 8(a)-(c) is that the atomic planes with slightly brighter intensity never exhibit an ordered arrangement of brighter spots corresponding to Gd-enriched atomic columns in the HAADF-STEM image and that the stacking of the hcp-type is not disturbed in the slightly brighter atomic planes. These observations indicate that the enrichment of Gd atoms occurs in four consecutive atomic planes to form either 6- or 7-layer structural blocks from the very beginning of the OD phase formation prior to the formation of Al_6Gd_8 clusters with the $L1_2$-type atomic arrangement introducing inevitably a stacking fault (fcc stacking) in the middle of the Gd-enriched four consecutive atomic planes.

The slightly brighter atomic planes enriched with Gd atoms without the disturbance of the stacking of the hcp type is similarly observed in the peripheral region of thicker OD precipitates, as typical examples of low-magnification and atomic-resolution HAADF-STEM images are shown in Figs. 7(b) and Fig. 8(d). This again confirms that the enrichment of Gd atoms in four consecutive atomic planes without disturbing the hcp stacking occurs as the initial stage of the thickening process of the OD precipitate along the stacking direction.

4.2.2. Intermediate stage of the formation processes of the OD intermetallic phase

An atomic-resolution HAADF-STEM image of a relatively thick OD precipitate (with the thickness of 0.5 μm) in the alloy annealed at 525 °C for 4 hours is shown in Fig. 9(a). The incident direction is [$1\bar{1}00$]. Judging from the ordered arrangement of 'double dagger' patterns of brighter spots in the four-consecutive central layers in each of 6-layer structural blocks, the long-range in-plane ordering of Al_6Gd_8 clusters is completed after annealing at 525 °C for 4 hours, as in the previous case (annealing at 400 °C for 10 hours) [13-15]. In Fig. 9(a), open circles indicate positions of Gd-enriched atomic columns in the outer layers of the Gd-enriched four consecutive atomic planes and numbers indicate the amount of the relative shift along the direction perpendicular to the stacking direction occurring between adjacent structural blocks expressed in the unit of the projected spacing between adjacent Gd-enriched columns in the outer layers of the four consecutive atomic planes (corresponding to the distance S_2 in Fig. 1(b)). Inspection of the relative shifts confirms that the C_1 stacking positions are preferred among three types of stacking positions (Fig. 1(b)) and that structural blocks do not exhibit any long-range stacking order in their stacking along the [0001] direction.

These characteristic features in the crystal structure of the OD phases are further confirmed by the coexistence of sharp and intense spots in the rows of the family reflections and sharp streaks in the rows of the characteristic reflections ($n/6[11\bar{2}l]$; $n = 6m+1$, $6m+2$, $6m+4$ and $6m+5$, m = integer, marked with arrows in Fig 9(c)) in SAED patterns shown in Figs. 9(b) and (c), respectively. Very weak streaks observed in the reciprocal lattice rows of the family reflections in Figs. 9(b) and (c) are due to minor incorporation of structural blocks composed of different numbers of close-packed planes.

4.2.3. Late stage of the formation processes of the OD intermetallic phase

Atomic-resolution HAADF-STEM images of a relatively large precipitate (with the thickness of 1.5 μm) of the OD intermetallic phase in the alloy annealed at 525 °C for 64 hours are shown in Figs. 10(a) and (b) for the incident beam directions [$2\bar{1}\bar{1}0$] and [$1\bar{1}00$], respectively. In addition to the long-range in-plane ordering in each structural block, a long-range ordering is confirmed to occur in the stacking of structural blocks by careful inspection of the relative shifts between adjacent structural blocks along directions perpendicular to the stacking direction. The relative shifts occurs exclusively by one third the projected spacing between adjacent Gd-enriched columns in the outer layers of the four consecutive atomic planes (corresponding to the distances S_1 and S_2 in Fig. 1(b) for [$2\bar{1}\bar{1}0$] and [$1\bar{1}00$] projections, respectively) in the same sense. The crystal structure of the OD intermetallic phase is thus confirmed to exhibit a tendency to transform into that of the simplest polytype of the MDO1 with a monoclinic cell (1*M*, space group: *C*2/*m*) after prolonged annealing at 525 °C for 64 hours. These two images correspond to those projected along [$1\bar{1}0$]$_{1M}$ and [$3\bar{1}0$]$_{1M}$ of the MDO1 polytype. Directions with a subscript 1*M* hereafter refer to those of the MDO1 polytype.

SAED patterns taken from the areas of Figs. 10(a) and (b) are shown in Figs. 10(c) and (d), respectively. In both SAED patterns, superlattice spots are observed in the 000*l* systematic row at positions dividing the distance between the transmitted beam and 0002 fundamental reflection by six, indicating that the number of close-packed atomic planes comprising each of structural blocks does not change during annealing at 525 °C at least up to 64 hours. This is in marked contrast to the case of LPSO phases in Mg-Zn-*RE* alloys, in which structural transformation from 18*R*-type (based on 6-layer structural blocks) to 14*H*-type (based on 7-layer structural blocks) is usually observed to

7

occur during annealing [4,9,12]. For the present OD phase, reciprocal lattice rows of the characteristic reflections pointed by arrows in the [1$\bar{1}$00] SAED pattern are converted from sharp streaks (in the as-cast state) to rows of intense discrete spots (Fig. 10(d)) after prolonged annealing. This is consistent with the result of the STEM observation of Fig. 10(b) that the crystal structure of the OD intermetallic phase with one-dimensional stacking disorder is converted to a fully ordered one. Positions of intense discrete diffraction spots in the SAED patterns of Figs. 10(c) and (d) match perfectly with those calculated for the MDO1 polytype with the incident beam directions $[110]_{1M}$ and $[010]_{1M}$, respectively. The MDO1 polytype is thus concluded to be the most energetically favourable among possible polytypes belonging to the OD-groupoid family described with the C_1 stacking position.

Although regions well within thick precipitates of the OD intermetallic phase is converted to a fully ordered MDO1 polytype, relatively thin precipitates as well as peripheral regions of thick precipitates often contain many different kinds of stacking irregularities, including intergrowth of different structural blocks. Figures 11(a) and (b) show a low-magnification bright-field TEM image of three thin precipitates (with the thickness of about 200 nm) and a low-magnification HAADF-STEM image of a peripheral region of a relatively thick precipitates (with the thickness of more than 1 μm), respectively. Structural blocks containing a larger number of Mg layers (mostly 7-layers) appear as bright lines in an OD precipitate seen in the central part of Fig. 11(a) and as dark lines in Fig. 11(b). An atomic-resolution HAADF image of the framed area in Fig. 11(b) clearly indicates that the ordered arrangement of the Gd-enriched columns is mostly perfect, except for a region where the transition from 6-layer structural blocks to 7-layer structural blocks occurs (Fig. 11(c)). These observations together with those of the nuclei of the OD phase (Figs. 6 and 7) suggest that the both 6-layer and 7-layer structural blocks are formed not only as the nuclei but also as the thickening process of pre-existing OD precipitates. As described above, structural blocks with atomic layer numbers different from six are eventually eliminated during annealing so that the most energetically favourable polytype (a fully ordered MDO1 polytype) consisting of 6-layer structural blocks finally appears. Since the elimination process of different structural blocks is expected to be caused by the movement of the transition regions observed in fig. 11(c), it is important to investigate the atomic scale structures of the transition regions for elucidating the elimination mechanism. Double dagger patterns of bright spots, which indicate the formation of the Al_6Gd_8 clusters with the $L1_2$-type atomic arrangement, are maintained and overlapped in the transition regions in fig. 11(c). Since the intensity of the bright spots in the double dagger patterns in the transition regions is relatively weak, the boundaries between two neighbouring structural blocks are considered to be inclined to the incident beam direction. These observations imply that the movement of the transition region can be interpreted as the local motion of the Al_6Gd_8 clusters. In the elimination process of 7-layer structural blocks, not only the shift of the Al_6Gd_8 clusters along the stacking direction to adjust the number of the atomic layer in the structural block but also their rotation to eliminate the twin-relation of the adjacent 7-layer structural blocks should be required [15]. Therefore, the elimination process of different structural block is inferred to be controlled mostly by a short-range diffusion process of the Al_6Gd_8 clusters.

8

5. Discussion

5.1. The stable crystal structure of the OD intermetallic phase

By considering some simple combinations of the stacking vectors (1a)-(1c), we can deduce some simple MDO polytypes for the 18R-type OD intermetallic compound in the Mg-Al-Gd system [14,15]. The simplest structure can be formed only with a single six-layer structural block by taking a monoclinic unit cell and the structure is expressed only with a single stacking vector, as follows.

$$\text{MDO1 polytype: } \boldsymbol{t}_i \ (i = 1, 2 \text{ or } 3) \tag{2a}$$

The stacking vector coincides with the c-axis of the monoclinic unit cell. The space group of the MDO1 (1M) polytype is $C2/m$. On the other hand, the second simplest structures can be formed by stacking two six-layer structural blocks with alternative selection of two of the three stacking vectors, as follows.

$$\text{MDO2 polytype: } \boldsymbol{t}_1 + \boldsymbol{t}_2 \text{ (equivalent to } \boldsymbol{t}_2 + \boldsymbol{t}_3 \text{ and } \boldsymbol{t}_3 + \boldsymbol{t}_1) \tag{2b}$$

The sum of the two stacking vectors corresponds to the c-axis of the monoclinic unit cell. The space group of the MDO2 (2M) polytype is $C2/c$. The third simplest structures can be formed by stacking three six-layer structural blocks with all three stacking vectors in a sequence, as follows.

$$\text{MDO3 polytype: } \boldsymbol{t}_1 + \boldsymbol{t}_2 + \boldsymbol{t}_3 \text{ (equivalent to } \boldsymbol{t}_2 + \boldsymbol{t}_3 + \boldsymbol{t}_1 \text{ and } \boldsymbol{t}_3 + \boldsymbol{t}_1 + \boldsymbol{t}_2) \tag{2b}$$

$$\text{MDO3' polytype: } \boldsymbol{t}_1 + \boldsymbol{t}_3 + \boldsymbol{t}_2 \text{ (equivalent to } \boldsymbol{t}_2 + \boldsymbol{t}_1 + \boldsymbol{t}_3 \text{ and } \boldsymbol{t}_3 + \boldsymbol{t}_2 + \boldsymbol{t}_1) \tag{2c}$$

The sum of the three stacking vectors is the c-axis of the unit cell of the trigonal system. The space group of these MDO3 and MDO3' (3T) polytypes are enantiomorphic and are $P3_112$ and $P3_212$, respectively.

  The present result indicates that the most energetically favourable polytype for the 18R-type OD intermetallic compound in the Mg-Al-Gd system is the MDO1 (1M) polytype (described with the stacking vector of (2a)) that is structurally the simplest one. Our preliminary results from first-principles calculations using the ab-initio total-energy and molecular dynamics program VASP (Vienna ab-initio simulation program) [27,28] support the conclusion that the structurally simplest polytype (MDO1 (1M)) has the lowest energy among other simplest polytypes for the 18R-type OD intermetallic compound in the Mg-Al-Gd system.

5.2. The formation processes of the OD intermetallic phase

The formation process of the most energetically favourable polytype (MDO1 (1M)) of the 18R-type OD intermetallic compound in the Mg-Al-Gd system can be summarized to occur in the following sequence.

(1) Enrichment of Gd (and possibly Al) in four consecutive close-packed planes while keeping the hcp stacking of the AB-type.
(2) The formation of Al_6Gd_8 clusters with the $L1_2$-type atomic arrangement in the four consecutive close-packed atomic planes, introducing a stacking fault (fcc-type stacking) in the middle of the four consecutive atomic planes.

(3) The thickening by the formation of Gd (and Al)-enrichment in four consecutive close-packed planes (i.e., the process (1)) at a distance of two or three close-packed Mg atomic planes high from the pre-existing Gd-enriched four consecutive atomic planes so as to form 6-layer (major) or 7-layer (minor) structural blocks.

(4) The in-plane ordering of Al_6Gd_8 clusters so that they occupy regularly the lattice points of the two-dimensional $2\sqrt{3}a_{Mg} \times 2\sqrt{3}a_{Mg}$ primitive hexagonal lattice and the stacking of structural blocks (OD layers) with the preferential stacking positions C_1 to form the OD structure.

(5) Elimination of different structural blocks (mostly 7-layer ones) and the long-range ordering in the stacking of structural blocks to form the structurally simplest MDO1 polytype.

The formation processes of the OD intermetallic phase in the Mg-Al-Gd system are also schematically illustrated in Fig. 12. One of the characteristic features in crystal structure of LPSO and OD phases in Mg-RE-TM systems is that the enrichment of RE (and TM) atoms occurs in four consecutive close-packed atomic planes in which a stacking fault that disturbs the hcp stacking of the AB-type occurs. The present study clearly indicates that the compositional modulation (the enrichment of RE (and TM) atoms) occurs prior to the introduction of a stacking fault in the hcp stacking of the AB-type. The introduction of stacking fault is evidently associated with the formation of Al_6Gd_8 clusters with the $L1_2$-type atomic arrangement in the four consecutive close-packed atomic planes. In contrast to many LPSO phases formed in the Mg-Zn-RE ternary systems (RE = Y, Dy, Ho, Er) that generally exhibit a structural transformation from 18R (6-layer structural block) to 14H (7-layer structural block) types upon annealing, the number of atomic planes in each of structural blocks for the OD phase in the Mg-Al-Gd system tends to converge into six, eliminating other structural blocks (mostly 7-layer ones) during annealing. This clearly indicates that crystal structures consisting of 6-layer structural blocks are energetically stable for OD intermetallic phases in the Mg-Al-Gd system. Our preliminary results indicate that this is also the case for most OD phases formed in the Mg-Al-RE ternary systems (RE = Y, Dy, Ho, Er).

Recently, TM_6RE_8 clusters are found to form also in Mg-Zn-RE LPSO phases [14,17], similarly in the present Mg-Al-Gd OD intermetallic phase. We believe that Mg-Zn-RE LPSO phases are formed also through the above processes (1), (2) and (3) in the early stage. However, the in-plane ordering of Zn_6RE_8 clusters do not occur usually in Mg-Zn-RE LPSO phases and the processes (4) and (5) are not therefore followed for their formation. Because of the absence of the in-plane ordering of Zn_6RE_8 clusters, a series of intermetallic phases formed in Mg-Zn-RE systems are called LPSO phase but not OD phase. We believe that the difference between the formation processes of OD phases in the Mg-Al-Gd system and that of LPSO phases in Mg-Zn-RE systems (i.e. whether or not the in-plane ordering occurs for Al_6Gd_8 or Zn_6RE_8 clusters) results from the different interaction strengths for Al_6Gd_8 clusters and Zn_6RE_8 clusters. The interaction strength is evidently much larger for Al_6Gd_8 clusters than for Zn_6RE_8 clusters in view of the occurrence of the in-plane ordering in the OD phase in the Mg-Al-Gd system. This is evident from the fact that for the OD phase in the Mg-Al-Gd system, the chemical composition of each structural block does not change so significantly during the thickening process and is considered to be quite close to the ideal one (Mg - 8.3 at.%Al - 11.1 at.%Gd) from the very initial stage of precipitation. Almost all lattice points of two-dimensional $2\sqrt{3}a_{Mg} \times 2\sqrt{3}a_{Mg}$ primitive hexagonal

lattice (Fig. 1(a)) are occupied by Al_6Gd_8 clusters all the time because of the strong interaction strength among the clusters. Indeed, the OD intermetallic phase in the Mg-Al-Gd system seems to form in a rather narrow composition range around the ideal one and no structural transformation, in which the number of atomic planes for structural blocks changes, occurs even upon annealing. On the other hand, LPSO phases in Mg-Zn-RE systems are generally reported to form in a much wider composition range [17]. We believe that this is a consequence from the weak interaction strength among Zn_6RE_8 clusters. When the Zn and RE concentrations in these LPSO phases are low (as usually reported), many of lattice points of two-dimensional $2\sqrt{3}a_{Mg} \times 2\sqrt{3}a_{Mg}$ primitive hexagonal lattice (or their equivalent positions in the absence of the in-plane ordering) in the LPSO structure are left unoccupied. Then, there is a possibility for phase transformation from 18*R*- to 14*H*-types to occur upon annealing by utilizing these unoccupied lattice points at which Zn_6RE_8 clusters to be allocated. The number density of Zn_6RE_8 clusters in each of the four consecutive atomic planes should increase while the Mg concentration in the consecutive planes should decrease to form an extra Mg plane in each of structural blocks during the 18*R*- to 14*H*-type phase transformation. When the Zn and RE concentrations in these LPSO phases are high, since most of lattice points for Zn_6RE_8 clusters to reside in the four consecutive planes are already occupied, phase transformation from 18*R*- to 14*H*-types seems to be very difficult to occur upon annealing. Very recently, it has been pointed out that the extent of the in-plane ordering depends on chemical composition in Mg-Zn-RE LPSO phases. A rather significant in-plane ordering is indeed observed if the composition is rich in Zn and RE [17]. Unfortunately, it is not yet known whether or not polytype transformation occurs also for the Mg-Zn-RE LPSO phase with the high Zn and RE concentrations.

6. Conclusions

(1) Of various possible polytypes that can be considered for for the 18*R*-type OD intermetallic compound (based on six-layer structural blocks) in the Mg-Al-Gd system in the framework of the OD theory, the most energetically favourable polytype is found to be the structurally simplest one, MDO1 (1*M*) polytype that is described with a single stacking vector in stacking six-layer structural blocks.

(2) The formation of the most energetically favourable polytype (MDO1 (1*M*)) of the 18*R*-type OD intermetallic compound in the Mg-Al-Gd system occurs in the sequence of (i) enrichment of Gd (and possibly Al) in four consecutive close-packed planes while keeping the hcp stacking of the AB-type, (ii) formation of Al_6Gd_8 clusters with the L1$_2$-type atomic arrangement in the four consecutive atomic planes, introducing a stacking fault in the middle of the four consecutive atomic planes, (iii) thickening by the formation of Gd (and Al)-enriched four consecutive planes at a distance of two or three close-packed Mg atomic planes high from the pre-existing Gd-enriched four consecutive atomic planes forming 6-layer (major) or 7-layer (minor) structural blocks, (iv) in-plane ordering of Al_6Gd_8 clusters in the four consecutive atomic planes and the stacking of structural blocks (OD layers) with the preferential stacking positions to form the OD structure, and (v) elimination of different structural blocks (other than 6-layer ones) and the long-range ordering in the stacking of structural blocks.

(3) The introduction of stacking fault in the four consecutive close-packed atomic planes is evidently associated with the formation of Al_6Gd_8 clusters with the L1$_2$-type atomic arrangement. The compositional modulation (the enrichment of

RE (and TM) atoms) is thus proved to occur in the hcp lattice prior to the introduction of a stacking fault.

Acknowledgements

References

1. Y. Kawamura, K. Hayashi, A. Inoue and T. Masumoto, Mater. Trans. 42 (2001) p.1172.
2. A. Inoue, Y. Kawamura, M. Matsushita, K. Hayashi and J. Koike, J. Mater. Res. 16 (2001) p.1894.
3. Y. Kawamura, T. Kasahara, S. Izumi and M. Yamasaki, Scripta Mater. 55 (2006) p.453.
4. Y. Kawamura and M. Yamasaki, Mater. Trans. 48 (2007) p.2986.
5. K. Hagihara, N. Yokotani and Y. Umakoshi, Intermetallics 18 (2010) p.267.
6. K. Hagihara, A. Kinoshita, Y. Sugino, M. Yamasaki, Y. Kawamura, H.Y. Yasuda and Y. Umakoshi, Acta Mater. 58 (2010) p.6282.
7. Z.P. Luo and S.Q. Zhang, J. Mater. Sci. Lett. 19 (2000), p.813.
8. D.H. Ping, K. Hono, Y. Kawamura and A. Inoue, Phil. Mag. Lett. 82 (2002) p.543.
9. T. Itoi, T. Seimiya, Y. Kawamura and M. Hirohashi, Scripta Mater. 51 (2004) p.107.
10. M. Matsuda, S. Ii, Y. Kawamura, Y. Ikuhara and M. Nishida, Mater. Sci. Eng. A393 (2005) p.269.
11. E. Abe, Y. Kawamura, K. Hayashi and A. Inoue, Acta Mater. 50 (2002), p.3845.
12. Y.M. Zhu, A.J. Morton and J.F. Nie, Acta Mater. 58 (2010) p.2936.
13. H. Yokobayashi, K. Kishida, H. Inui, M. Yamasaki and Y. Kawamura, Mater. Res. Soc. Symp. Proc., 1295 (2011) p.267.
14. H. Yokobayashi, K. Kishida, H. Inui, M. Yamasaki and Y. Kawamura, Acta Mater. 59 (2011) p.7287.
15. K. Kishida, H. Yokobayashi, H. Inui, M. Yamasaki and Kawamura, Intermetallics 31 (2012) p.55 .
16. E. Abe, A. Ono, T. Itoi, M. Yamasaki and Y. Kawamura, Philos. Mag. Lett. 91 (2011) p.690.
17. D. Egusa, E. Abe, Acta Mater., 60 (2012) p.166.
18. K. Dornberger-Schiff, Acta Cryst. 9 (1956) p.593.
19. K. Dornberger-Schiff and H. Grell-Niemann, Acta Cryst. 14 (1961) p.167.
20. K. Dornberger-Schiff, Abh. Dtsch. Akad. Wiss. Berlin, Kl. Chem. Geol. Biol. 3 (1964) p.1.
21. K. Dornberger-Schiff and K. Fichtner, Krist. Tech. 7 (1972) p.1035.
22. S. Ďurovič, *Fundamentals of the OD theory*, in *Modular aspects of minerals / EMU Notes in Mineralogy, Vol. 1*, S. Merlino ed., Eötvös University Press, Budapest, 1999, p.1.
23. S. Merlino, *OD approach in minerals: examples and applications*, in *Modular aspects of minerals / EMU Notes in Mineralogy, Vol. 1*, S. Merlino ed., Eötvös University Press, Budapest, 1999, p.29.
24. G. Ferraris, E. Makovicky and S. Merlino, *Crystallography of Modular Materials*,

Oxford University Press, New York, 2004.
25. V. Kopský and D.B. Litvin DB (eds.), *International Table for Crystallography, Vol. E, second ed.*, John Wiley & Sons, Ltd., West Sussex, 2010.
26. R. Kilaas, *Interactive simulation of high resolution electron micrographs*, in *Proc 45th Ann Meeting EMSA*, G.W. Bailey ed, San Francisco Press, San Francisco, 1987, p.66.
27. G. Kresse, J. Furthmüller, Phys. Rev. B, 54 (1996) p.11169.
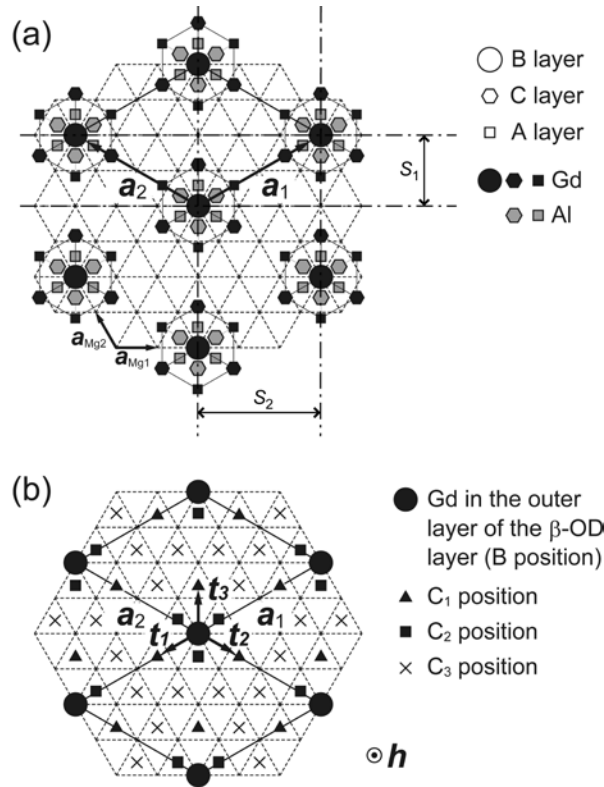28. G. Kresse, D. Joubert, Phys. Rev. B, 59 (1999) p.1758.

Figure 1. (a) Periodic arrangement of Al_6Gd_8 clusters with the $L1_2$-type atomic arrangement in the quadruple layers in the OD layer of the $18R$-type Mg-Al-Gd OD intermetallic phase projected along [0001]. (b) Possible stacking positions of the β-OD layer (stacking sequence: BCBACA) stacked on the α-OD layer (stacking sequence: ABACBC). Positions of α- and β-OD layers are indicated with those of the Gd atoms in the outer Gd-enriched atomic layers in the B and C positions, respectively.
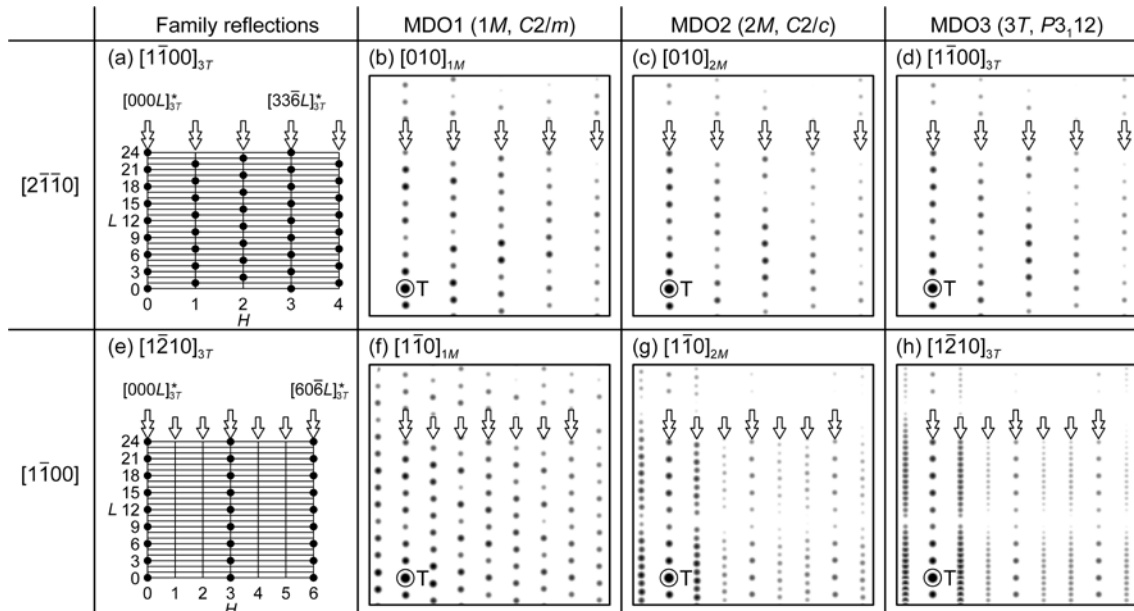
Figure 2. Calculated SAED patterns for the $18R$-type Mg-Al-Gd OD intermetallic phase in the $[2\bar{1}\bar{1}0]$ and $[1\bar{1}00]$ projections. (a,e) family reflections, (b-d, f-h) calculated for three MDO polytypes $1M$, $2M$ and $3T$. Two-headed and one-headed arrows indicate the reciprocal lattice rows of the family and characteristic reflections, respectively.

14
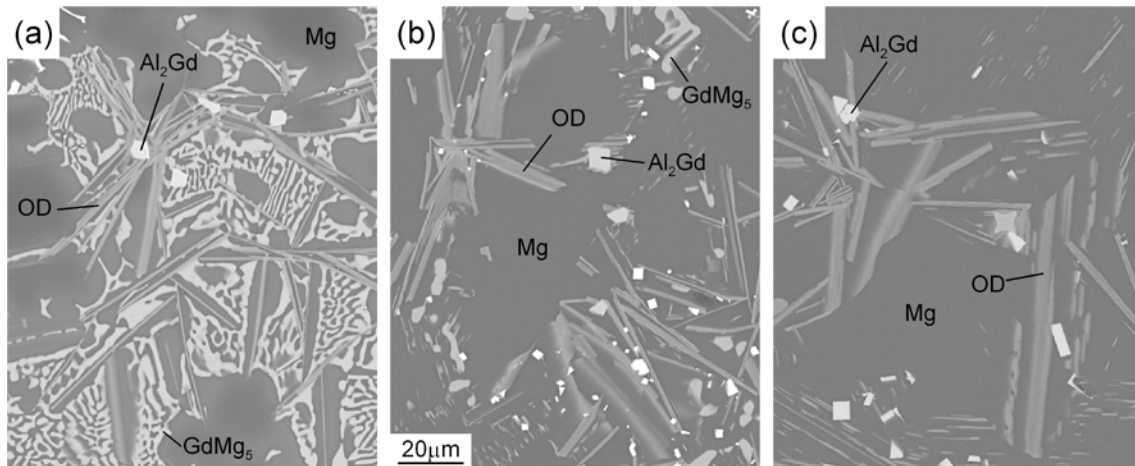
Figure 3. SEM backscattered electron images of (a) the as-solidified ingot, (b) the ingot annealed at 525 °C for 4 hours and (c) the ingot annealed at 525 °C for 64 hours.
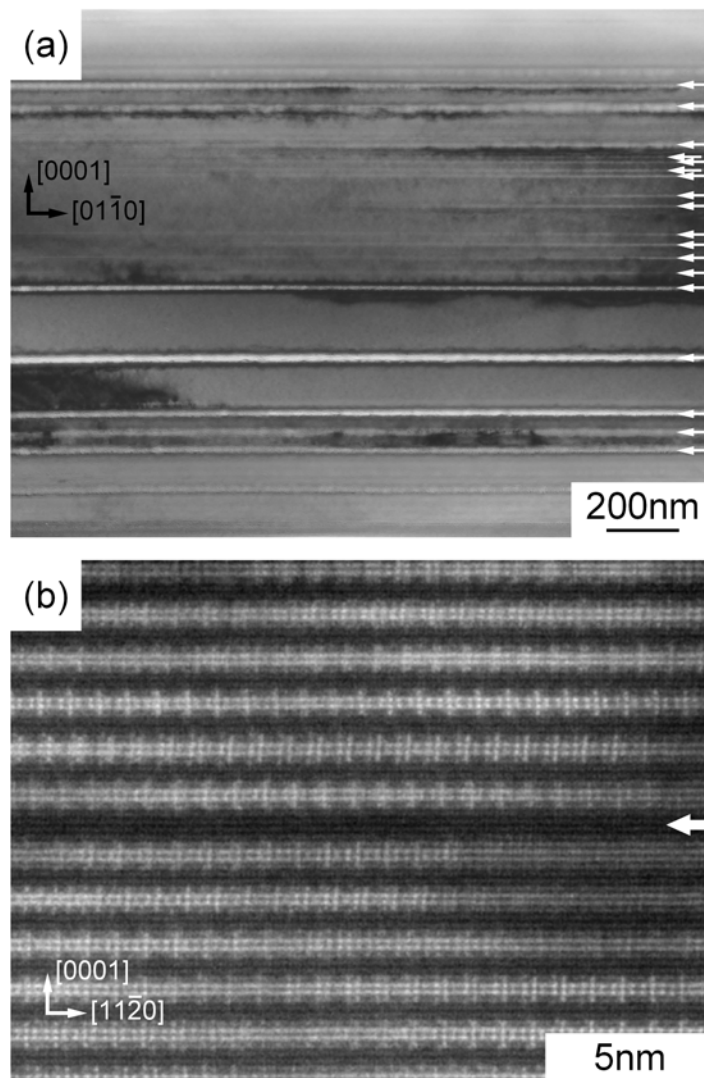
Figure 4. (a) A low-magnification bright-field (BF)-TEM image and (b) an atomic-resolution HAADF-STEM image of OD intermetallic precipitates in the as-solidified ingots. Arrows indicate positions with stacking irregularity.
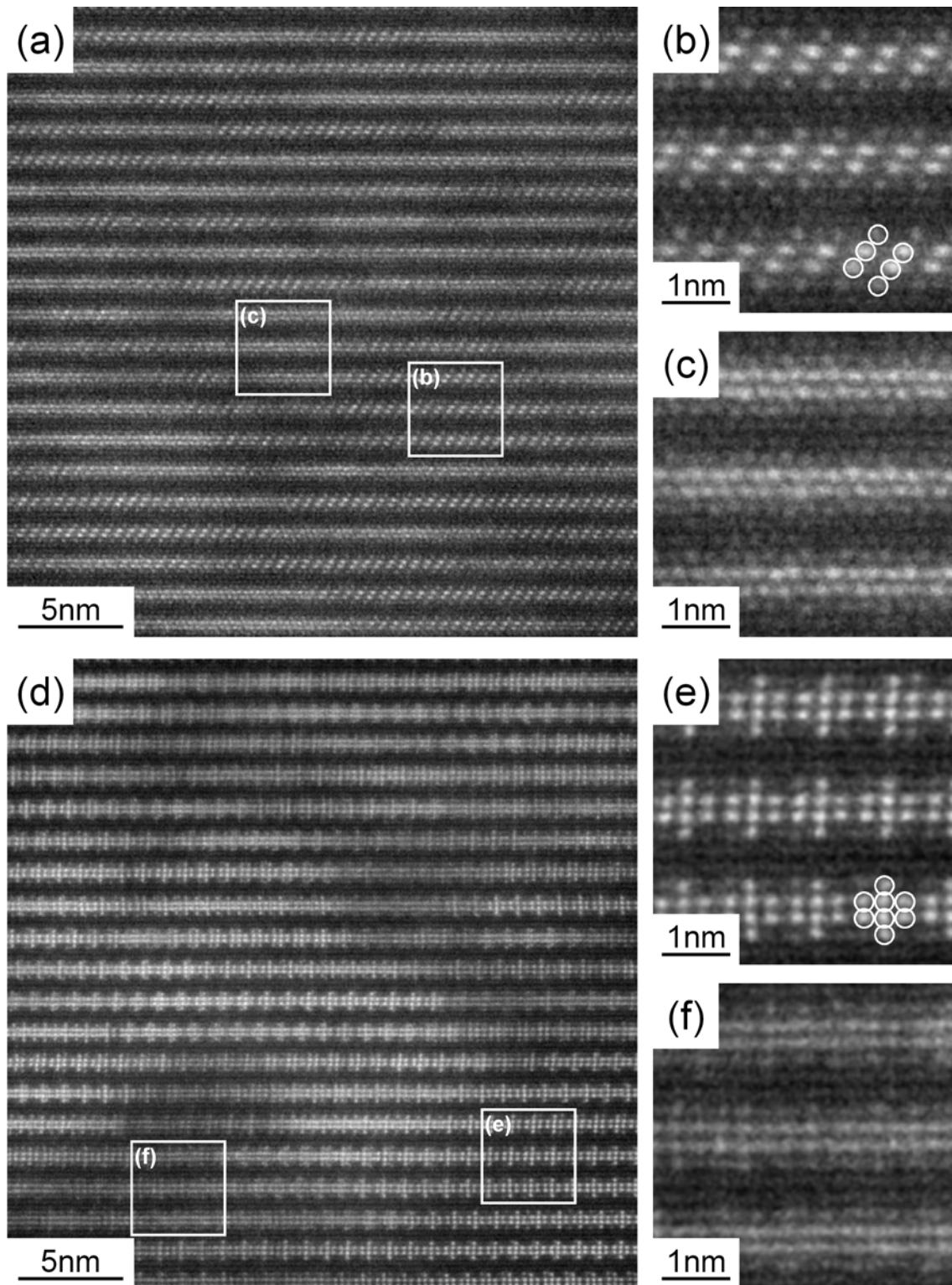
Figure 5. Atomic resolution HAADF-STEM images of 18*R*-type stacking regions composed of the 6 atomic-layer structural blocks in the central parts of relatively thick OD intermetallic precipitates in the as-solidified ingots taken along (a-c) [2$\bar{1}\bar{1}$0] and (d-f) [1$\bar{1}$00].
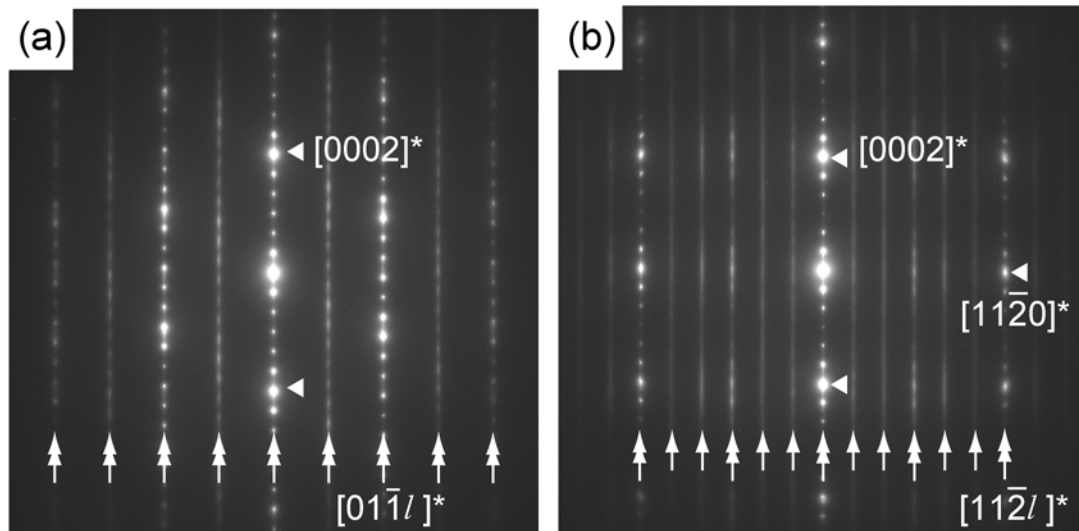
Figure 6. SAED patterns of the Mg-Al-Gd OD intermetallic precipitate in the as-solidified ingot taken along (a) $[2\bar{1}\bar{1}0]$ and (b) $[1\bar{1}00]$. Two-headed and one-headed arrows indicate the reciprocal lattice rows of the family and characteristic reflections, respectively.
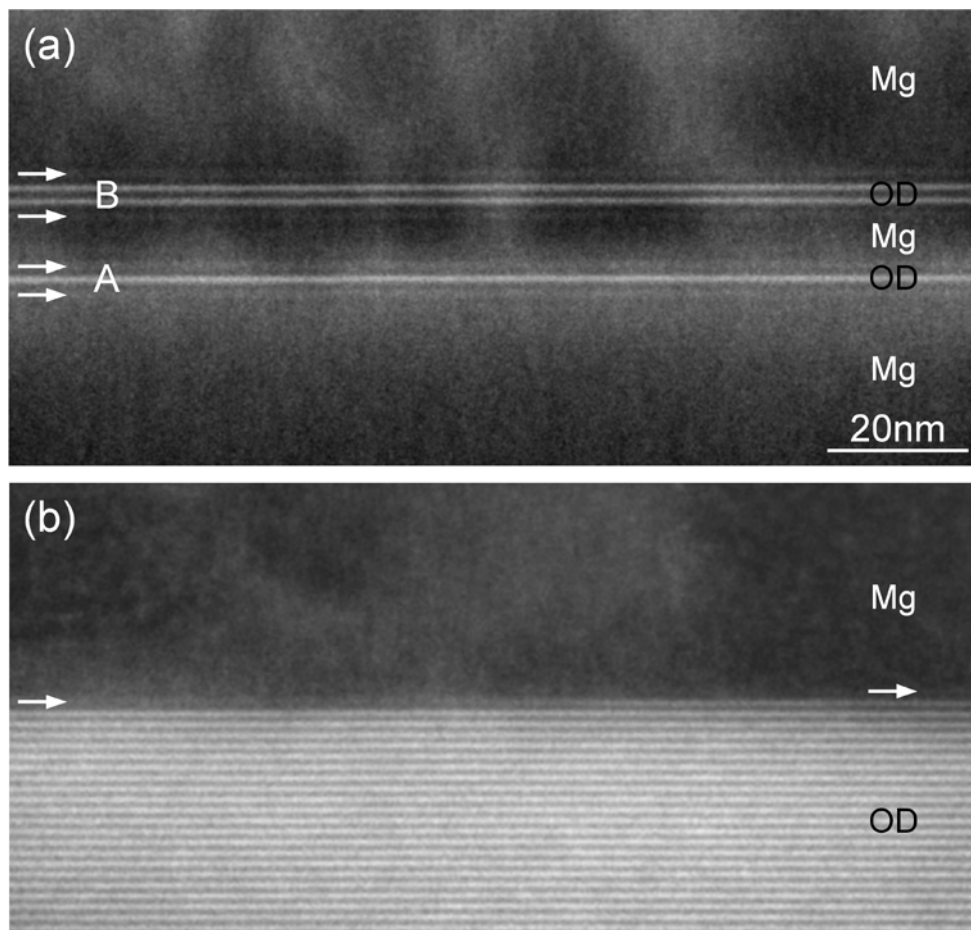
Figure 7. Low-magnification HAADF-STEM images of (a) a region containing very thin precipitates of the OD intermetallic phase and (b) a peripheral region of a relatively thick precipitate in the as-solidified ingot. Arrows indicates the positions of faint lines corresponding to slightly Gd and Al- enriched atomic layers.
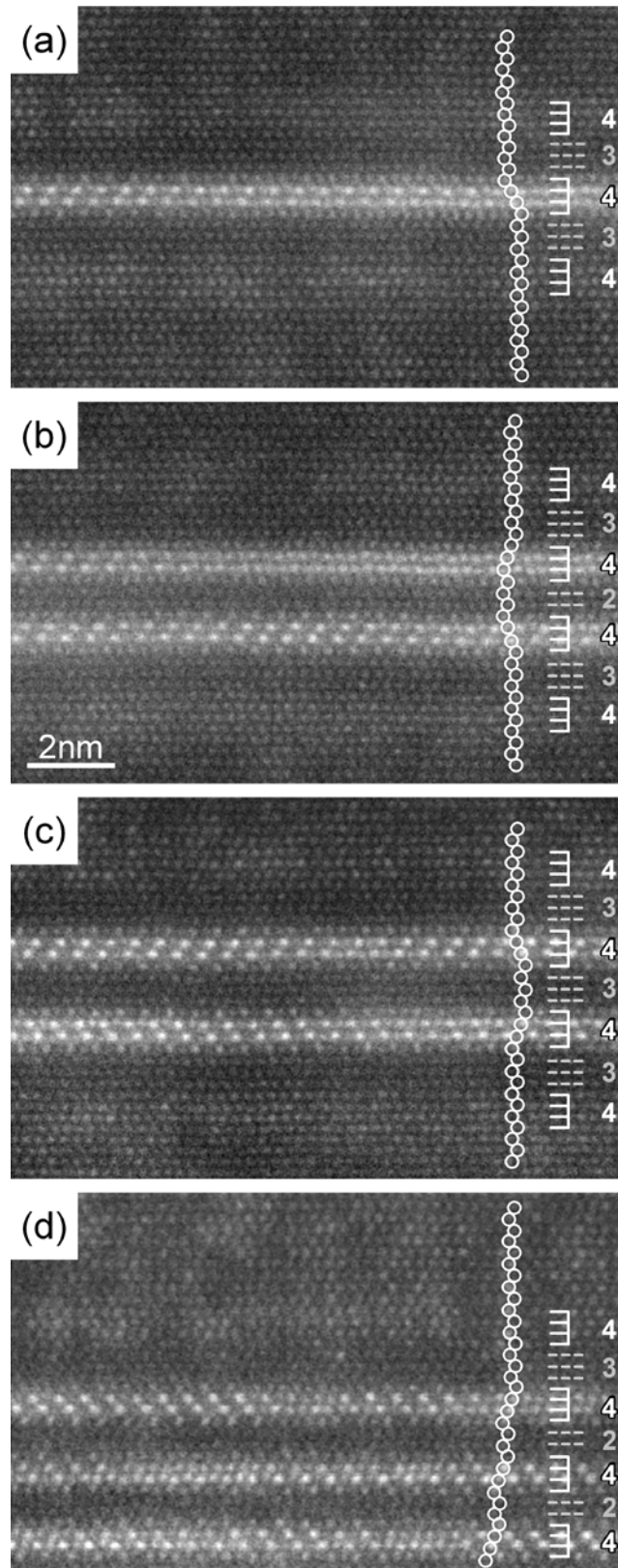
Figure 8. Atomic-resolution HAADF-STEM images taken along [2$\bar{1}\bar{1}$0] of (a-c) very thin OD precipitates and (d) a peripheral region of a relatively thick precipitate in the as-solidified ingot. Dashed lines and numbers in gray colour indicate positions and numbers of the Mg atomic planes. White lines and numbers indicate positions and numbers of the Gd-enriched atomic planes.
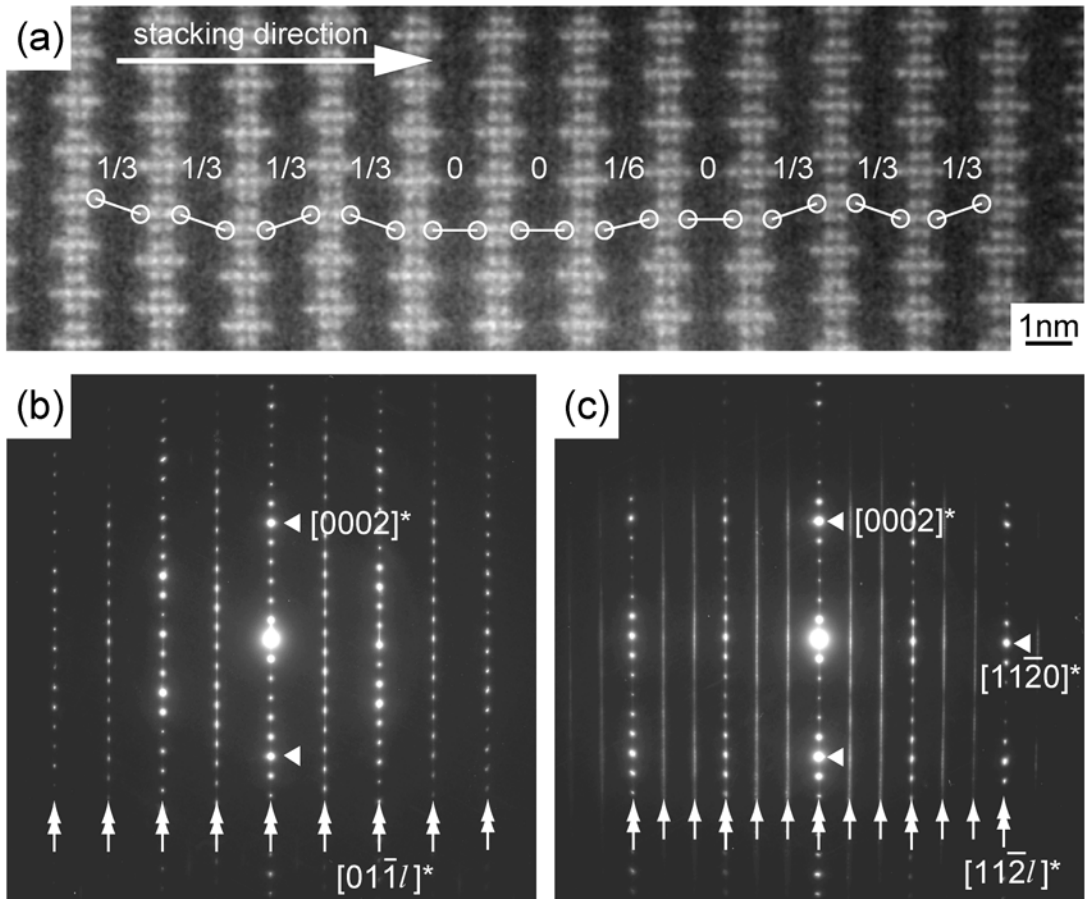
Figure 9. (a) An atomic-resolution HAADF-STEM image and (b,c) SAED patterns of OD intermetallic precipitates in the alloy annealed at 525 °C for 4 hours. The incident beam directions are (a,c) [1$\bar{1}$00] and (b) [2$\bar{1}\bar{1}$0]. Numbers in (a) indicate the amount of the relative shift between adjacent OD layers in the unit of the projected spacing between adjacent Gd-enriched columns in the outer layers of the Gd-enriched four consecutive atomic planes. Two-headed and one-headed arrows in (b,c) indicate the reciprocal lattice rows of the family and characteristic reflections, respectively.
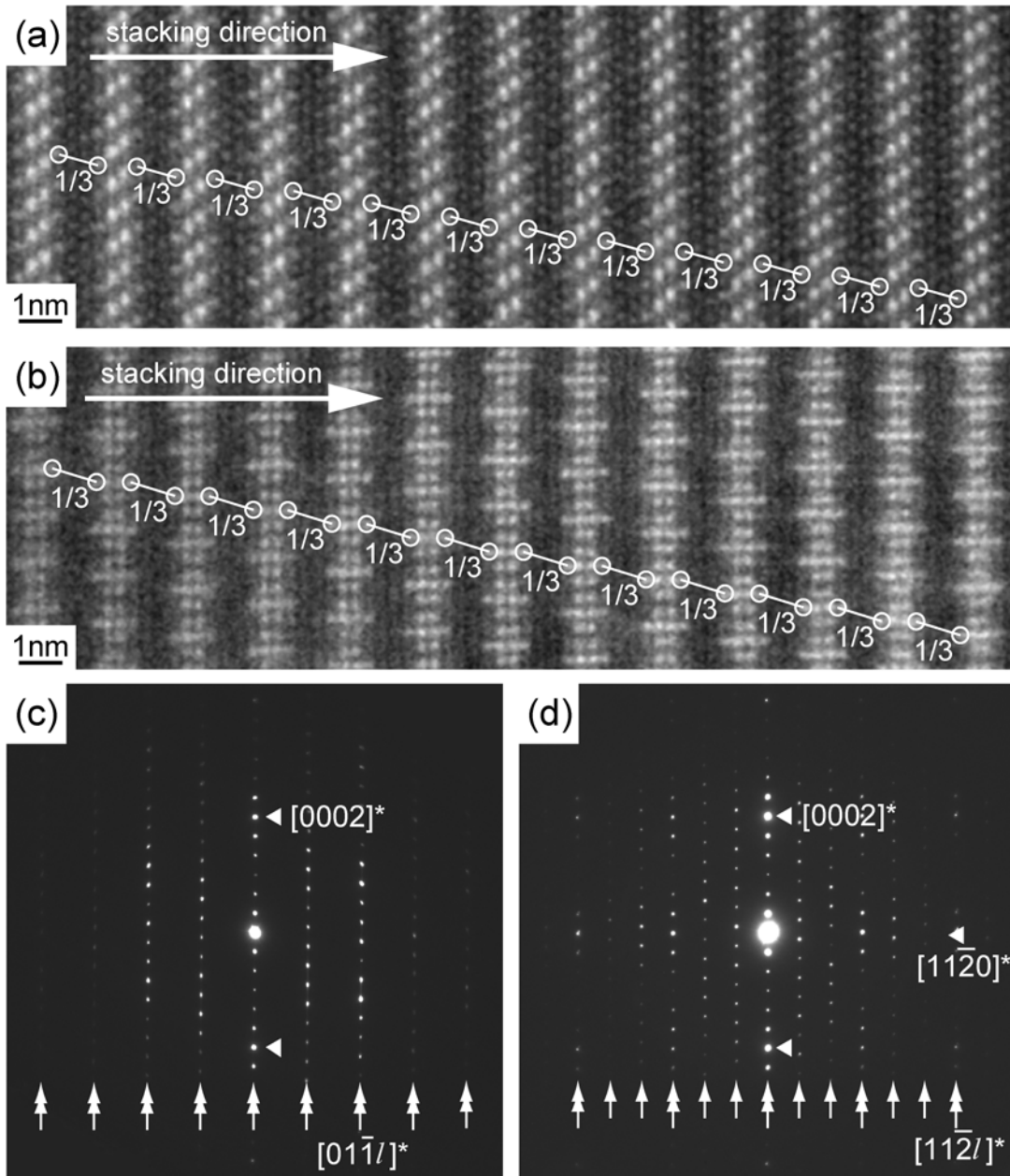
Figure 10. (a,b) Atomic-resolution HAADF-STEM images and (c,d) SAED patterns of OD intermetallic precipitates in the alloy annealed at 525 °C for 64 hours. The incident beam directions are (a,c) [2$\bar{1}\bar{1}$0] and (b,d) [1$\bar{1}$00]. Numbers in (a,b) indicate the amount of the relative shift between adjacent OD layers in the unit of the projected spacing between adjacent Gd-enriched columns in the outer layers of the Gd-enriched four consecutive atomic planes. Two-headed and one-headed arrows in (c,d) indicate the reciprocal lattice rows of the family and characteristic reflections, respectively.
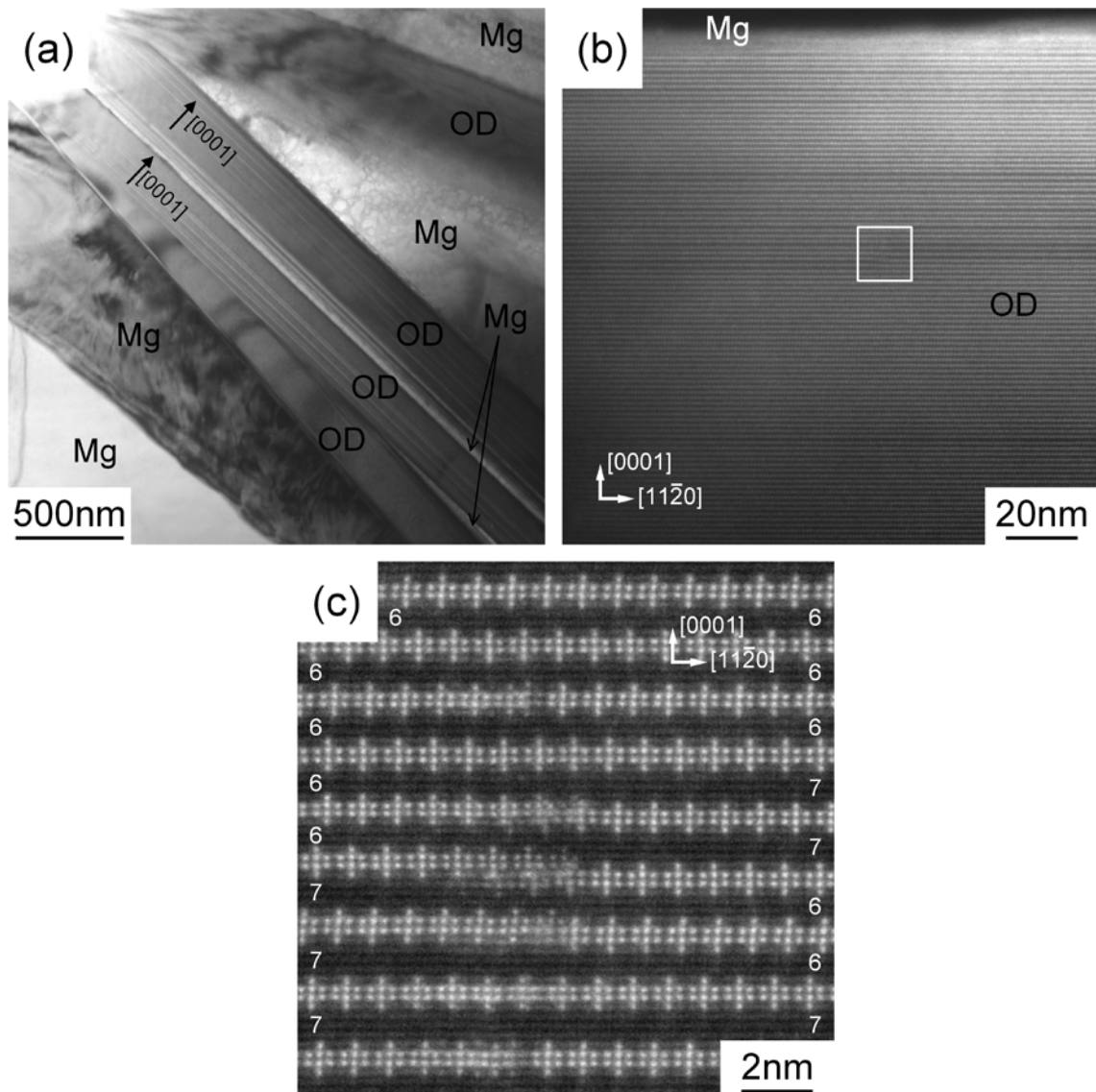
20

Figure 11. (a) A low-magnification bright-field TEM image of three thin precipitates (with the thickness of about 200 nm) and (b) A low-magnification HAADF-STEM image of a peripheral region of a relatively thick precipitates (with a thickness of more than 1 μm) in the alloy annealed at 525 °C for 64 hours. (c) An Atomic resolution HAADF-STEM image of the squared region in (b).
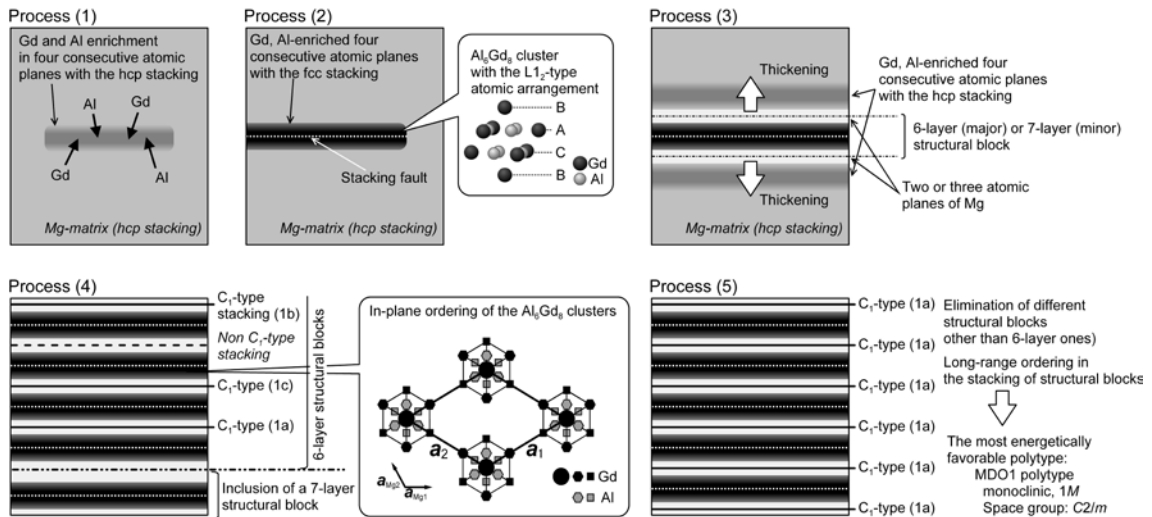
Figure 12. Schematic illustration of the formation processes of the OD intermetallic phase in the Mg-Al-Gd system.